

# SUSY-QCD corrections to scalar quark decays into charginos and neutralinos

S. Kraml<sup>1</sup>, H. Eberl<sup>1</sup>,  
 A. Bartl<sup>2</sup>, W. Majerotto<sup>1</sup>, W. Porod<sup>2</sup>

(1) *Institut für Hochenergiephysik, Österreichische Akademie der Wissenschaften,  
 Vienna, Austria*

(2) *Institut für Theoretische Physik, Universität Wien, Vienna, Austria*

## Abstract

We calculate the supersymmetric  $\mathcal{O}(\alpha_s)$  QCD corrections to the decays  $\tilde{q}_i \rightarrow q' \tilde{\chi}_j^\pm$  ( $i, j = 1, 2$ ) and  $\tilde{q}_i \rightarrow q \tilde{\chi}_k^0$  ( $k = 1, \dots, 4$ ) within the Minimal Supersymmetric Standard Model. In particular we consider the decays of squarks of the third generation,  $\tilde{t}_i$  and  $\tilde{b}_i$  ( $i = 1, 2$ ), where the left-right mixing must be taken into account. The corrections turn out to be of about 10%, except for higgsino-like charginos or neutralinos, where they can go up to 40%.

# 1 Introduction

In supersymmetry (SUSY) [1] every quark has two scalar partners, the squarks  $\tilde{q}_L$  and  $\tilde{q}_R$ . Quite generally,  $\tilde{q}_L$  and  $\tilde{q}_R$  mix giving the mass eigenstates  $\tilde{q}_1$  and  $\tilde{q}_2$  (with  $m_{\tilde{q}_1} < m_{\tilde{q}_2}$ ). Whereas the mixing can be neglected for the partners of the light quarks, it can be important for the third generation due to the Yukawa coupling which is proportional to  $m_t$  or  $m_b$  [2].

In the case that the gluino is heavier than the squarks, the squarks have the decay modes  $\tilde{q}_{1,2} \rightarrow q' \tilde{\chi}_j^\pm$  ( $j = 1, 2$ ), and  $\tilde{q}_{1,2} \rightarrow q \tilde{\chi}_k^0$  ( $k = 1, \dots, 4$ ), where  $\tilde{\chi}_j^\pm$  and  $\tilde{\chi}_k^0$  denote the charginos and neutralinos, respectively. These decays were discussed so far only on the basis of tree-level calculations, for the partners of the light quarks in ref. [3] and with inclusion of the third generation ( $\tilde{t}_i, \tilde{b}_i, i = 1, 2$ ) in ref. [4]. A detailed study of the  $\tilde{t}_i$  and  $\tilde{b}_i$  decays can be found in [5, 6].

Here we calculate the  $\mathcal{O}(\alpha_s)$  QCD corrections (including the exchange of SUSY particles) to these decays within the Minimal Supersymmetric Standard Model (MSSM). In particular, we do not neglect the masses of quarks and take into account  $\tilde{q}_L$ - $\tilde{q}_R$  mixing, so that the formulae are also applicable to the decays  $\tilde{t}_i \rightarrow b \tilde{\chi}_j^+$ ,  $\tilde{t}_i \rightarrow t \tilde{\chi}_j^0$ , and  $\tilde{b}_i \rightarrow t \tilde{\chi}_j^-$ ,  $\tilde{b}_i \rightarrow b \tilde{\chi}_j^0$ . We work in the on-shell renormalization scheme. For the renormalization of the squark mixing angle we use the scheme introduced in [7], where we applied it to the case of  $e^+e^- \rightarrow \tilde{q}_i \tilde{q}_j^*$ . We also give a numerical analysis of the QCD corrections to the decays  $\tilde{t}_i \rightarrow b \tilde{\chi}_j^-$  and  $\tilde{t}_i \rightarrow t \tilde{\chi}_k^0$ .

For the decays of a squark into a light quark ( $m_q = 0$ ) and a photino the SUSY-QCD corrections were already calculated in [8]. The QCD corrections to the decay  $t \rightarrow \tilde{t}_i \tilde{\chi}_k^0$  have been computed very recently within the MSSM in ref. [9]. The SUSY-QCD corrections to the strong decays  $\tilde{q} \rightarrow q \tilde{g}$  were calculated in ref. [10].

## 2 Tree level formulae

The squarks  $\tilde{q}_L$  and  $\tilde{q}_R$  are related to the mass eigenstates  $\tilde{q}_1$  and  $\tilde{q}_2$  by:

$$\begin{pmatrix} \tilde{q}_1 \\ \tilde{q}_2 \end{pmatrix} = \mathcal{R}^{\tilde{q}} \begin{pmatrix} \tilde{q}_L \\ \tilde{q}_R \end{pmatrix}, \quad \mathcal{R}^{\tilde{q}} = \begin{pmatrix} \cos \theta_{\tilde{q}} & \sin \theta_{\tilde{q}} \\ -\sin \theta_{\tilde{q}} & \cos \theta_{\tilde{q}} \end{pmatrix}. \quad (1)$$

Their interaction with charginos  $\tilde{\chi}_j^\pm$  ( $j = 1, 2$ ) and neutralinos  $\tilde{\chi}_k^0$  ( $k = 1, \dots, 4$ ) is given by [5]:

$$\mathcal{L} = g \bar{q} (a_{ik}^{\tilde{q}} P_R + b_{ik}^{\tilde{q}} P_L) \tilde{\chi}_k^0 \tilde{q}_i + g \bar{t} (\ell_{ij}^{\tilde{b}} P_R + k_{ij}^{\tilde{b}} P_L) \tilde{\chi}_j^+ \tilde{b}_i + g \bar{b} (\ell_{ij}^{\tilde{t}} P_R + k_{ij}^{\tilde{t}} P_L) \chi_j^{+c} \tilde{t}_i + \text{h.c.} \quad (2)$$

$q$ ,  $t$ ,  $b$ ,  $\tilde{\chi}_j^+$ , and  $\tilde{\chi}_k^0$  denote the four-component spinors of the corresponding particles. The respective decay widths at tree level are

$$\Gamma^0(\tilde{q}_i \rightarrow q' \tilde{\chi}_j^\pm) = \frac{g^2 \lambda^{\frac{1}{2}}(m_{\tilde{q}_i}^2, m_{q'}^2, m_{\tilde{\chi}_j^\pm}^2)}{16\pi m_{\tilde{q}_i}^3} \left( [(\ell_{ij}^{\tilde{q}})^2 + (k_{ij}^{\tilde{q}})^2] X - 4 \ell_{ij}^{\tilde{q}} k_{ij}^{\tilde{q}} m_{q'} m_{\tilde{\chi}_j^\pm} \right) \quad (3)$$

and

$$\Gamma^0(\tilde{q}_i \rightarrow q \tilde{\chi}_k^0) = \frac{g^2 \lambda^{\frac{1}{2}}(m_{\tilde{q}_i}^2, m_q^2, m_{\tilde{\chi}_k^0}^2)}{16\pi m_{\tilde{q}_i}^3} \left( [(a_{ik}^{\tilde{q}})^2 + (b_{ik}^{\tilde{q}})^2] X' - 4 a_{ik}^{\tilde{q}} b_{ik}^{\tilde{q}} m_q m_{\tilde{\chi}_k^0} \right) \quad (4)$$

where  $\lambda(x, y, z) = x^2 + y^2 + z^2 - 2xy - 2xz - 2yz$  and

$$X = m_{\tilde{q}_i}^2 - m_{q'}^2 - m_{\tilde{\chi}_j^\pm}^2, \quad X' = m_{\tilde{q}_i}^2 - m_q^2 - m_{\tilde{\chi}_k^0}^2. \quad (5)$$

The  $\tilde{q}_i$ - $q'$ - $\tilde{\chi}_j^\pm$  couplings  $\ell_{ij}^{\tilde{q}}$  and  $k_{ij}^{\tilde{q}}$  are

$$\ell_{ij}^{\tilde{q}} = \mathcal{R}_{in}^{\tilde{q}} \mathcal{O}_{jn}^q, \quad k_{ij}^{\tilde{q}} = \mathcal{R}_{i1}^{\tilde{q}} \mathcal{O}_{j2}^{q'} \quad (6)$$

with

$$\mathcal{O}_j^t = \begin{pmatrix} -V_{j1} \\ Y_t V_{j2} \end{pmatrix}, \quad \mathcal{O}_j^b = \begin{pmatrix} -U_{j1} \\ Y_b U_{j2} \end{pmatrix}. \quad (7)$$

The  $\tilde{q}_i$ - $q$ - $\tilde{\chi}_k^0$  couplings  $a_{ik}^{\tilde{q}}$  and  $b_{ik}^{\tilde{q}}$  are given by

$$a_{ik}^{\tilde{q}} = \mathcal{R}_{in}^{\tilde{q}} \mathcal{A}_{kn}^q, \quad b_{ik}^{\tilde{q}} = \mathcal{R}_{in}^{\tilde{q}} \mathcal{B}_{kn}^q \quad (8)$$

with

$$\mathcal{A}_k^q = \begin{pmatrix} f_{Lk}^q \\ h_{Rk}^q \end{pmatrix}, \quad \mathcal{B}_k^q = \begin{pmatrix} h_{Lk}^q \\ f_{Rk}^q \end{pmatrix}, \quad (9)$$

and

$$\begin{aligned} h_{Lk}^t &= Y_t (N_{k3} \sin \beta - N_{k4} \cos \beta), & f_{Lk}^t &= -\frac{2\sqrt{2}}{3} \sin \theta_W N_{k1} - \sqrt{2} \left( \frac{1}{2} - \frac{2}{3} \sin^2 \theta_W \right) \frac{N_{k2}}{\cos \theta_W}, \\ h_{Rk}^t &= Y_t (N_{k3} \sin \beta - N_{k4} \cos \beta), & f_{Rk}^t &= -\frac{2\sqrt{2}}{3} \sin \theta_W (\tan \theta_W N_{k2} - N_{k1}), \end{aligned} \quad (10)$$

$$\begin{aligned} h_{Lk}^b &= -Y_b (N_{k3} \cos \beta + N_{k4} \sin \beta), & f_{Lk}^b &= \frac{\sqrt{2}}{3} \sin \theta_W N_{k1} + \sqrt{2} \left( \frac{1}{2} - \frac{1}{3} \sin^2 \theta_W \right) \frac{N_{k2}}{\cos \theta_W}, \\ h_{Rk}^b &= -Y_b (N_{k3} \cos \beta + N_{k4} \sin \beta), & f_{Rk}^b &= \frac{\sqrt{2}}{3} \sin \theta_W (\tan \theta_W N_{k2} - N_{k1}). \end{aligned} \quad (11)$$

$N_{ij}$  is the  $4 \times 4$  unitary matrix diagonalizing the neutral gaugino–higgsino mass matrix in the basis  $\tilde{\gamma}, \tilde{Z}^0, \tilde{H}_1^0 \cos \beta - \tilde{H}_2^0 \sin \beta, \tilde{H}_1^0 \sin \beta + \tilde{H}_2^0 \cos \beta$  [1, 11].  $U_{ij}$  and  $V_{ij}$  are the  $2 \times 2$  unitary matrices diagonalizing the charged gaugino–higgsino mass matrix [1, 12]. Assuming CP conservation, we choose a phase convention in which  $N_{ij}$ ,  $U_{ij}$ , and  $V_{ij}$  are real.  $Y_f$  denotes the Yukawa coupling,

$$Y_t = m_t/(\sqrt{2} m_W \sin \beta), \quad Y_b = m_b/(\sqrt{2} m_W \cos \beta). \quad (12)$$

### 3 SUSY–QCD corrections

The  $\mathcal{O}(\alpha_s)$  SUSY–QCD corrected decay width can be decomposed in the following way:

$$\Gamma = \Gamma^0 + \delta\Gamma^{(v)} + \delta\Gamma^{(w)} + \delta\Gamma^{(c)} + \delta\Gamma_{g,real}. \quad (13)$$

The superscript  $v$  denotes the vertex correction (Figs. 1b, c),  $w$  the wave function correction (Figs. 1d–h), and  $c$  the shift from the bare to the on-shell couplings.  $\delta\Gamma_{g,real}$  is the correction due to real gluon emission (Figs. 1i, 1j) which has to be included in order to achieve infrared finiteness. According to eq. (3)  $\delta\Gamma^{(a)}$  ( $a = v, w, c$ ) can be written as

$$\begin{aligned} \delta\Gamma^{(a)}(\tilde{q}_i \rightarrow q' \tilde{\chi}_j^\pm) = & \frac{g^2 \lambda^{\frac{1}{2}}(m_{\tilde{q}_i}^2, m_{q'}^2, m_{\tilde{\chi}_j^\pm}^2)}{16\pi m_{\tilde{q}_i}^3} \\ & \left[ (2 \ell_{ij}^{\tilde{q}} \delta\ell_{ij}^{\tilde{q}(a)} + 2 k_{ij}^{\tilde{q}} \delta k_{ij}^{\tilde{q}(a)}) X - 4 m_{q'} m_{\tilde{\chi}_j^\pm} (\ell_{ij}^{\tilde{q}} \delta k_{ij}^{\tilde{q}(a)} + k_{ij}^{\tilde{q}} \delta\ell_{ij}^{\tilde{q}(a)}) \right] \end{aligned} \quad (14)$$

with  $X$  as defined in eq. (5). An analogous expression holds for  $\delta\Gamma^{(a)}(\tilde{q}_i \rightarrow q \tilde{\chi}_k^0)$  by replacing  $\tilde{\chi}_j^\pm \rightarrow \tilde{\chi}_k^0$ ,  $q' \rightarrow q$ ,  $X \rightarrow X'$ ,  $\ell_{ij}^{\tilde{q}} \rightarrow a_{ik}^{\tilde{q}}$ ,  $k_{ij}^{\tilde{q}} \rightarrow b_{ik}^{\tilde{q}}$ ,  $\delta\ell_{ij}^{\tilde{q}(a)} \rightarrow \delta a_{ik}^{\tilde{q}(a)}$ , and  $\delta k_{ij}^{\tilde{q}(a)} \rightarrow \delta b_{ik}^{\tilde{q}(a)}$ .  $\delta\ell_{ij}^{\tilde{q}(a)}$ ,  $\delta k_{ij}^{\tilde{q}(a)}$ , etc. get contributions from gluon exchange, gluino exchange, and the four–squark interaction. As we will see, in the renormalization scheme used the four–squark interaction contribution turns out to be zero.

In what follows we will take the squark decays into charginos as example. For the decays  $\tilde{q}_i \rightarrow q \tilde{\chi}_k^0$  one has to make the replacements just mentioned before.

### 3.1 Vertex corrections

The gluonic vertex correction (Fig. 1b) yields

$$\delta \ell_{ij}^{\tilde{q}(v,g)} = \frac{\alpha_s}{3\pi} \left\{ [(4m_{q'}^2 + 2X)(C_0 + C_1 + C_2) + (2m_{\tilde{\chi}_j^\pm}^2 + X)C_1 + B_0] \ell_{ij}^{\tilde{q}} \right. \\ \left. + [2m_{q'} m_{\tilde{\chi}_j^\pm} C_2] k_{ij}^{\tilde{q}} \right\}, \quad (15)$$

$$\delta k_{ij}^{\tilde{q}(v,g)} = \frac{\alpha_s}{3\pi} \left\{ [(4m_{q'}^2 + 2X)(C_0 + C_1 + C_2) + (2m_{\tilde{\chi}_j^\pm}^2 + X)C_1 + B_0] k_{ij}^{\tilde{q}} \right. \\ \left. + [2m_{q'} m_{\tilde{\chi}_j^\pm} C_2] \ell_{ij}^{\tilde{q}} \right\}. \quad (16)$$

$B_0$ ,  $C_0$ ,  $C_1$ , and  $C_2$  are the standard two- and three-point functions [13]. In this case,  $B_0 = B_0(m_{\tilde{\chi}_j^\pm}^2, m_{\tilde{q}_i}^2, m_{q'}^2)$  and  $C_m = C_m(m_{\tilde{q}_i}^2, m_{\tilde{\chi}_j^\pm}^2, m_{q'}^2; \lambda^2, m_{\tilde{q}_i}^2, m_{q'}^2)$ , where we follow the conventions of [14]. As usually, we introduce a gluon mass  $\lambda$  for the regularization of infrared divergencies.

The contribution to the vertex correction due to the graph shown in Fig. 1c with a gluino and a squark  $\tilde{q}'_n$  ( $n = 1, 2$ ) in the loop is:

$$\delta \ell_{ij}^{\tilde{q}(v,\tilde{g})} = \frac{2}{3} \frac{\alpha_s}{\pi} \left\{ m_{\tilde{\chi}_j^\pm} [(m_{q'} \alpha_{LR} + m_q \alpha_{RL} - m_{\tilde{g}} \alpha_{LL}) \ell_{nj}^{\tilde{q}'} + m_{\tilde{\chi}_j^\pm} \alpha_{RL} k_{nj}^{\tilde{q}'}] C_1 \right. \\ \left. + m_{q'} [(m_{q'} \alpha_{RL} - m_q \alpha_{LR} + m_{\tilde{g}} \alpha_{RR}) k_{nj}^{\tilde{q}'} - m_{\tilde{\chi}_j^\pm} \alpha_{LR} \ell_{nj}^{\tilde{q}'}] (C_1 + C_2) \right. \\ \left. + m_{\tilde{g}} [(m_{q'} \alpha_{RR} - m_q \alpha_{LL} + m_{\tilde{g}} \alpha_{RL}) k_{nj}^{\tilde{q}'} - m_{\tilde{\chi}_j^\pm} \alpha_{LL} \ell_{nj}^{\tilde{q}'}] C_0 + (XC_1 + B_0) \alpha_{RL} k_{nj}^{\tilde{q}'} \right\}, \quad (17)$$

$$\delta k_{ij}^{\tilde{q}(v,\tilde{g})} = \frac{2}{3} \frac{\alpha_s}{\pi} \left\{ m_{\tilde{\chi}_j^\pm} [(m_{q'} \alpha_{RL} + m_q \alpha_{LR} - m_{\tilde{g}} \alpha_{RR}) k_{nj}^{\tilde{q}'} + m_{\tilde{\chi}_j^\pm} \alpha_{LR} \ell_{nj}^{\tilde{q}'}] C_1 \right. \\ \left. + m_{q'} [(m_{q'} \alpha_{LR} - m_q \alpha_{RL} + m_{\tilde{g}} \alpha_{LL}) \ell_{nj}^{\tilde{q}'} - m_{\tilde{\chi}_j^\pm} \alpha_{RL} k_{nj}^{\tilde{q}'}] (C_1 + C_2) \right. \\ \left. + m_{\tilde{g}} [(m_{q'} \alpha_{LL} - m_q \alpha_{RR} + m_{\tilde{g}} \alpha_{LR}) \ell_{nj}^{\tilde{q}'} - m_{\tilde{\chi}_j^\pm} \alpha_{RR} k_{nj}^{\tilde{q}'}] C_0 + (XC_1 + B_0) \alpha_{LR} \ell_{nj}^{\tilde{q}'} \right\} \quad (18)$$

with

$$\alpha_{LL} = (\alpha_{LL})_{in} = \mathcal{R}_{i1}^{\tilde{q}} \mathcal{R}_{n1}^{\tilde{q}'}, \quad \alpha_{LR} = (\alpha_{LR})_{in} = \mathcal{R}_{i1}^{\tilde{q}} \mathcal{R}_{n2}^{\tilde{q}'}, \\ \alpha_{RL} = (\alpha_{RL})_{in} = \mathcal{R}_{i2}^{\tilde{q}} \mathcal{R}_{n1}^{\tilde{q}'}, \quad \alpha_{RR} = (\alpha_{RR})_{in} = \mathcal{R}_{i2}^{\tilde{q}} \mathcal{R}_{n2}^{\tilde{q}'}. \quad (19)$$

Here,  $B_0 = B_0(m_{\tilde{\chi}_j^\pm}^2, m_{\tilde{q}'_n}^2, m_q^2)$ , and  $C_m = C_m(m_{\tilde{q}_i}^2, m_{\tilde{\chi}_j^\pm}^2, m_{q'}^2; m_{\tilde{g}}^2, m_{\tilde{q}'_n}^2, m_q^2)$ .

### 3.2 Wave-function correction

The wave-function correction is given by

$$\delta \ell_{ij}^{\tilde{q}(w)} = \frac{1}{2} [\delta Z_{q'}^{L\dagger} + \delta \tilde{Z}_{ii}] \ell_{ij}^{\tilde{q}} + \delta \tilde{Z}_{ii'} \ell_{i'j}^{\tilde{q}}, \quad (20)$$

$$\delta k_{ij}^{\tilde{q}(w)} = \frac{1}{2} [\delta Z_{q'}^{R\dagger} + \delta \tilde{Z}_{ii}] k_{ij}^{\tilde{q}} + \delta \tilde{Z}_{ii'} k_{i'j}^{\tilde{q}}. \quad (21)$$

$Z_{q'}^{L,R}$  are the quark wave-function renormalization constants due to gluon exchange (Fig. 1d),

$$\delta Z_{q'}^{L\dagger(g)} = \delta Z_{q'}^{R\dagger(g)} = -\frac{2}{3} \frac{\alpha_s}{\pi} [B_0 + B_1 - 2m_{q'}^2(\dot{B}_0 - \dot{B}_1) - r/2] \quad (22)$$

with  $B_m = B_m(m_{q'}^2, \lambda^2, m_{q'}^2)$ ,  $\dot{B}_m = \dot{B}_m(m_{q'}^2, \lambda^2, m_{q'}^2)$ , and due to gluino exchange (Fig. 1e),

$$\delta Z_{q'}^{L\dagger(\tilde{g})} = \frac{2}{3} \frac{\alpha_s}{\pi} \left\{ \cos^2 \theta_{\tilde{q}'} B_1^1 + \sin^2 \theta_{\tilde{q}'} B_1^2 + m_{q'}^2 [\dot{B}_1^1 + \dot{B}_1^2 + \frac{2m_{\tilde{g}}}{m_{q'}} \sin 2\theta_{\tilde{q}'} (\dot{B}_0^1 - \dot{B}_0^2)] \right\}, \quad (23)$$

$$\delta Z_{q'}^{R\dagger(\tilde{g})} = \frac{2}{3} \frac{\alpha_s}{\pi} \left\{ \sin^2 \theta_{\tilde{q}'} B_1^1 + \cos^2 \theta_{\tilde{q}'} B_1^2 + m_{q'}^2 [\dot{B}_1^1 + \dot{B}_1^2 + \frac{2m_{\tilde{g}}}{m_{q'}} \sin 2\theta_{\tilde{q}'} (\dot{B}_0^1 - \dot{B}_0^2)] \right\}, \quad (24)$$

where  $B_m^i = B_m(m_{q'}^2, m_{\tilde{g}}^2, m_{q_i'}^2)$  and  $\dot{B}_m^i = \dot{B}_m(m_{q'}^2, m_{\tilde{g}}^2, m_{q_i'}^2)$ . The parameter  $r$  in eq. (22) and eq. (32) exhibits the dependence on the regularization. As  $r$  does not cancel in the final result we have to use the dimensional reduction scheme [15] ( $r = 0$ ) which preserves supersymmetry at least at one-loop order.

The squark wave-function renormalization constants  $\tilde{Z}_{in}$  stem from gluon, gluino, and squark loops according to Figs. 1f – 1h. They are given by:

$$\delta \tilde{Z}_{ii}^{(g,\tilde{g})} = -\text{Re} \left\{ \dot{\Sigma}_{ii}^{(g,\tilde{g})}(m_{\tilde{q}_i}^2) \right\}, \quad \delta \tilde{Z}_{ii'}^{(\tilde{g},\tilde{q})} = -\frac{\text{Re} \left\{ \Sigma_{ii'}^{(\tilde{g},\tilde{q})}(m_{\tilde{q}_i}^2) \right\}}{m_{\tilde{q}_i}^2 - m_{\tilde{q}_{i'}}^2}, \quad i \neq i' \quad (25)$$

with  $\dot{\Sigma}_{ii}(m^2) = \partial \Sigma_{ii}(p^2) / \partial p^2|_{p^2=m^2}$ . The squark self-energy contribution due to gluon exchange (Fig. 1f) is

$$\begin{aligned} \dot{\Sigma}_{ii}^{(g)}(m_{\tilde{q}_i}^2) &= -\frac{\alpha_s}{3\pi} \left\{ 3B_0(m_{\tilde{q}_i}^2, 0, m_{\tilde{q}_i}^2) + 2B_1(m_{\tilde{q}_i}^2, 0, m_{\tilde{q}_i}^2) \right. \\ &\quad \left. + 4m_{\tilde{q}_i}^2 \dot{B}_0(m_{\tilde{q}_i}^2, \lambda^2, m_{\tilde{q}_i}^2) + 2m_{\tilde{q}_i}^2 \dot{B}_1(m_{\tilde{q}_i}^2, 0, m_{\tilde{q}_i}^2) \right\}, \end{aligned}$$

and that due to gluino exchange (Fig. 1g) is

$$\begin{aligned} \dot{\Sigma}_{ii}^{(\tilde{g})}(m_{\tilde{q}_i}^2) &= \frac{2}{3} \frac{\alpha_s}{\pi} \left[ B_0(m_{\tilde{q}_i}^2, m_{\tilde{g}}^2, m_q^2) + (m_{\tilde{q}_i}^2 - m_q^2 - m_{\tilde{g}}^2) \dot{B}_0(m_{\tilde{q}_i}^2, m_{\tilde{g}}^2, m_q^2) \right. \\ &\quad \left. - 2m_q m_{\tilde{g}} (-1)^i \sin 2\theta_{\tilde{q}} \dot{B}_0(m_{\tilde{q}_i}^2, m_{\tilde{g}}^2, m_q^2) \right], \end{aligned} \quad (26)$$

$$\Sigma_{12}^{(\tilde{g})}(m_{\tilde{q}_i}^2) = \Sigma_{21}^{(\tilde{g})}(m_{\tilde{q}_i}^2) = \frac{4}{3} \frac{\alpha_s}{\pi} m_{\tilde{g}} m_q \cos 2\theta_{\tilde{q}} B_0(m_{\tilde{q}_i}^2, m_{\tilde{g}}^2, m_q^2). \quad (27)$$

The four-squark interaction (Fig. 1h) gives

$$\Sigma_{12}^{(\tilde{q})}(m_{\tilde{q}_i}^2) = \Sigma_{21}^{(\tilde{q})}(m_{\tilde{q}_i}^2) = \frac{\alpha_s}{6\pi} \sin 4\theta_{\tilde{q}} [A_0(m_{\tilde{q}_2}^2) - A_0(m_{\tilde{q}_1}^2)] \quad (28)$$

where  $A_0(p^2)$  is the standard one-point function in the convention of [14]. Note that  $\Sigma_{ii'}^{(\tilde{q})}(p^2)$  is independent of  $p^2$  and hence  $\Sigma_{ii'}^{(\tilde{q})}(m_{\tilde{q}_1}^2) = \Sigma_{ii'}^{(\tilde{q})}(m_{\tilde{q}_2}^2) = \Sigma_{ii'}^{(\tilde{q})}$ .

### 3.3 Renormalization of the bare couplings

In order to make the shift from the bare to the on-shell couplings it is necessary to renormalize the quark mass as well as the squark mixing angle:

$$\delta \ell_{ij}^{\tilde{q}(c)} = \mathcal{S}_{in}^{\tilde{q}} \mathcal{O}_{jn}^q \delta \theta_{\tilde{q}} + \mathcal{R}_{i2}^{\tilde{q}} \delta \mathcal{O}_{j2}^q, \quad \delta k_{ij}^{\tilde{q}(c)} = \mathcal{S}_{i1}^{\tilde{q}} \mathcal{O}_{j2}^{q'} \delta \theta_{\tilde{q}} + \mathcal{R}_{i1}^{\tilde{q}} \delta \mathcal{O}_{j2}^{q'}, \quad (29)$$

$$\delta a_{ik}^{\tilde{q}(c)} = \mathcal{S}_{in}^{\tilde{q}} \mathcal{A}_{kn}^q \delta \theta_{\tilde{q}} + \mathcal{R}_{i2}^{\tilde{q}} \delta h_{Rk}^q, \quad \delta b_{ik}^{\tilde{q}(c)} = \mathcal{S}_{in}^{\tilde{q}} \mathcal{B}_{kn}^q \delta \theta_{\tilde{q}} + \mathcal{R}_{i1}^{\tilde{q}} \delta h_{Lk}^q, \quad (30)$$

where

$$\mathcal{S}^{\tilde{q}} \delta \theta_{\tilde{q}} = \delta \mathcal{R}^{\tilde{q}} = \begin{pmatrix} -\sin \theta_{\tilde{q}} & \cos \theta_{\tilde{q}} \\ -\cos \theta_{\tilde{q}} & -\sin \theta_{\tilde{q}} \end{pmatrix} \delta \theta_{\tilde{q}}. \quad (31)$$

$\delta \mathcal{O}_{j2}^t = V_{j2}/(\sqrt{2} m_W \sin \beta) \delta m_t$ ,  $\delta \mathcal{O}_{j2}^b = U_{j2}/(\sqrt{2} m_W \cos \beta) \delta m_b$ , and analogously for  $\delta h_{Lk}^q$  and  $\delta h_{Rk}^q$  according to eqs. (10) – (12). The gluon contribution to  $\delta m_q$  is

$$\delta m_q^{(g)} = -\frac{2}{3} \frac{\alpha_s}{\pi} m_q [B_0 - B_1 - r/2], \quad B_m = B_m(m_q^2, 0, m_q^2), \quad (32)$$

and the gluino contribution is

$$\delta m_q^{(\tilde{g})} = -\frac{\alpha_s}{3\pi} [m_q(B_1^1 + B_1^2) + m_{\tilde{g}} \sin 2\theta_{\tilde{q}}(B_0^1 - B_0^2)], \quad B_m^i = B_m(m_q^2, m_{\tilde{g}}^2, m_{\tilde{q}_i}^2). \quad (33)$$

For the renormalization of the squark mixing angle we use the scheme introduced in [7]:

$$\delta \theta_{\tilde{q}}^{(\tilde{q})} = \frac{\alpha_s}{6\pi} \frac{\sin 4\theta_{\tilde{q}}}{m_{\tilde{q}_1}^2 - m_{\tilde{q}_2}^2} [A_0(m_{\tilde{q}_2}^2) - A_0(m_{\tilde{q}_1}^2)]. \quad (34)$$

$$\delta \theta_{\tilde{q}}^{(\tilde{g})} = \frac{\alpha_s}{3\pi} \frac{m_{\tilde{g}} m_q}{I_q^3(m_{\tilde{q}_1}^2 - m_{\tilde{q}_2}^2)} [B_0(m_{\tilde{q}_2}^2, m_{\tilde{g}}^2, m_q^2) \tilde{v}_{11} - B_0(m_{\tilde{q}_1}^2, m_{\tilde{g}}^2, m_q^2) \tilde{v}_{22}]. \quad (35)$$

with  $\tilde{v}_{ih}$  the  $Z\tilde{q}_i\tilde{q}_h^*$  couplings,  $\tilde{v}_{11} = 4(I_q^{3L} \cos^2 \theta_{\tilde{q}} - s_W^2 e_q)$  and  $\tilde{v}_{22} = 4(I_q^{3L} \sin^2 \theta_{\tilde{q}} - s_W^2 e_q)$ . Here  $I_q^{3L}$  is the third component of the weak isospin and  $e_q$  the charge of the quark  $q$ .

With this choice of  $\delta\theta_{\tilde{q}}$  the squark contribution to the correction is zero:  $\delta\Gamma^{(w,\tilde{q})} + \delta\Gamma^{(c,\tilde{q})} = 0$ . Moreover, the off-diagonal contribution ( $i \neq h$ ) of Fig. 1g vanishes in this scheme. We checked analytically that the resulting SUSY-QCD corrected decay width is ultraviolet finite.

### 3.4 Real gluon emission

The  $\mathcal{O}(\alpha_s)$  contribution from real gluon emission, as shown in Figs. 1i and 1j, gives the decay width of  $\tilde{q}_i \rightarrow g q' \tilde{\chi}_j^\pm$ :

$$\begin{aligned} \Gamma(\tilde{q}_i \rightarrow g q' \tilde{\chi}_j^\pm) = & -\frac{g^2 \alpha_s}{6\pi^2 m_{\tilde{q}_i}} \left\{ [(k_{ij}^{\tilde{q}})^2 + (\ell_{ij}^{\tilde{q}})^2] (I_1^0 + I) + \right. \\ & \left. 2Z [m_{\tilde{q}_i}^2 I_{00} + m_{q'}^2 I_{11} + (m_{\tilde{q}_i}^2 + m_{q'}^2 - m_{\tilde{\chi}_j^\pm}^2) I_{01} + I_0 + I_1] \right\} \quad (36) \end{aligned}$$

where  $Z = [(k_{ij}^{\tilde{q}})^2 + (\ell_{ij}^{\tilde{q}})^2]X - 4k_{ij}^{\tilde{q}}\ell_{ij}^{\tilde{q}}m_{q'}m_{\tilde{\chi}_j^\pm}$ . The phase space integrals  $I$ ,  $I_n$ ,  $I_{nm}$ , and  $I_n^m$  have  $(m_{\tilde{q}_i}, m_{q'}, m_{\tilde{\chi}_j^\pm})$  as arguments and are given in [14]. An analogous expression holds for the  $\tilde{q}_i \rightarrow g q \tilde{\chi}_k^0$  decay width.

## 4 Numerical results and discussion

We now turn to the numerical analysis of the  $\mathcal{O}(\alpha_s)$  SUSY-QCD corrected decay widths. As examples we consider the decays  $\tilde{t}_1 \rightarrow b \tilde{\chi}_1^+$  and  $\tilde{t}_1 \rightarrow t \tilde{\chi}_1^0$ . Masses and couplings of the charginos and neutralinos depend on the parameters  $M$ ,  $M'$ ,  $\mu$ , and  $\tan \beta$ . The squark sector is determined by the soft-breaking parameters  $M_Q$ ,  $M_U$ , and  $M_D$ , the trilinear couplings  $A_t$  and  $A_b$ , and  $\mu$  and  $\tan \beta$ , which all enter the squark mass matrices. For the following analysis we use physical squark masses and mixing angles as input parameters. We take  $m_t = 180$  GeV,  $m_b = 5$  GeV,  $m_Z = 91.187$  GeV,  $\sin^2 \theta_W = 0.23$ ,  $\alpha_w(m_Z) = 1/128.87$ , and  $\alpha_s(m_Z) = 0.12$ . Moreover, we use the GUT relations  $M' = \frac{5}{3} M \tan^2 \theta_W \sim 0.5M$  and  $m_{\tilde{g}} = \frac{\alpha_s}{\alpha_2} M \sim 0.3M$ . Furthermore, we use  $\alpha_s(Q^2) = 4\pi/(b_0 x) [1 - 2b_1 \ln x/(b_0^2 x)]$  with  $b_0 = 11 - 2/3 n_f$ ,  $b_1 = 51 - 19/3 n_f$ , and  $x = \ln(Q^2/\Lambda^2)$  [16]. Here,  $n_f$  is the number of flavours.



For discussing the  $\tilde{t}_1 \rightarrow b \tilde{\chi}_1^+$  decay mode we take  $m_{\tilde{\chi}_1^\pm} = 75$  GeV,  $m_{\tilde{t}_2} = 300$  GeV,  $m_{\tilde{b}_1} = 220$  GeV,  $m_{\tilde{b}_2} = 230$  GeV,  $\cos \theta_{\tilde{t}} = -0.4$ , and  $\tan \beta = 2$ . In order to study the dependence on the nature of the chargino (gaugino- or higgsino-like), we choose three sets of  $M$  and  $\mu$  values:  $M \ll |\mu|$  ( $M = 66$  GeV,  $\mu = -500$  GeV),  $M \sim |\mu|$  ( $M = 70$  GeV,  $\mu = -61$  GeV), and  $M \gg |\mu|$  ( $M = 300$  GeV,  $\mu = -62$  GeV). In Fig. 2 we show the dependence of the QCD corrections on the  $\tilde{t}_1$  mass (in % of the tree-level decay width) in the range of  $m_{\tilde{t}_1} = 80$  GeV (LEP2, Tevatron) to  $m_{\tilde{t}_1} = 220$  GeV (LHC,  $e^+e^-$  linear collider). Here, we take  $\cos \theta_{\tilde{t}} = 0.72$  which corresponds to  $M_Q \sim M_U$ . If the  $\tilde{\chi}_1^+$  is gaugino-like (solid line) the correction is about 10% to 20% for a light  $\tilde{t}_1$  ( $m_{\tilde{t}_1} \lesssim 100$  GeV) and decreases with the stop mass. In the case of  $M \sim |\mu|$  (dashed line) the correction lies between  $\sim +10\%$  and  $-10\%$ . Due to the large top Yukawa coupling the biggest effect is found for a higgsino-like  $\tilde{\chi}_1^+$  (dash-dotted line). Here, the correction lies in the range of -20% to -40%.

The  $\cos \theta_{\tilde{t}}$  dependence is shown in Fig. 3 where we plot the  $\mathcal{O}(\alpha_s)$  corrected decay widths (solid lines) together with the tree-level widths (dashed lines) as a function of  $\cos \theta_{\tilde{t}}$  for  $m_{\tilde{t}_1} = 150$  GeV and the other parameters as given above. The widths show the characteristic dependence on the stop mixing angle: If  $\tilde{t}_1 \sim \tilde{t}_R$  ( $\cos \theta_{\tilde{t}} \sim 0$ ) it strongly couples to the higgsino component of  $\tilde{\chi}_1^+$ , whereas for  $\tilde{t}_1 \sim \tilde{t}_L$  ( $\cos \theta_{\tilde{t}} \sim \pm 1$ ) it strongly couples to the gaugino component. Again, a striking effect can be seen for  $|\mu| \ll M$ . However, also for  $M \ll |\mu|$  and  $M \sim |\mu|$  the correction can be larger than 10%, especially if the tree-level decay width is very small.

We have also studied the dependence on the masses and the mixing angle of the exchanged sbottom (Fig. 1c). In the cases studied these effects turn out to be small. The dependence on the gluino mass is more complex: On the one hand, the gluino mass enters in the propagator of the graphs in Figs. 1c, 1e, and 1g. On the other hand, the mass and the couplings of  $\tilde{\chi}_1^+$  in the final state also depend on  $m_{\tilde{g}}$  via the relation  $M \sim 0.3 m_{\tilde{g}}$ . However, if one relaxes this relation keeping  $M$  fixed and varying  $m_{\tilde{g}}$  the correction increases with the gluino mass. This has also been noticed in refs. [8, 9].

For the decay of  $\tilde{t}_1$  into  $t \tilde{\chi}_1^0$  we take  $m_{\tilde{\chi}_1^0} = 50$  GeV,  $m_{\tilde{t}_2} = 400$  GeV,  $m_{\tilde{b}_1} = 320$  GeV,  $m_{\tilde{b}_2} = 340$  GeV,  $\cos \theta_{sb} = -0.4$ , and  $\tan \beta = 2$ . Again, we choose scenarios with a gaugino-like  $\tilde{\chi}_1^0$  ( $M = 98$  GeV,  $\mu = -500$  GeV) and a higgsino-like  $\tilde{\chi}_1^0$  ( $M = 250$  GeV,  $\mu = -55$  GeV), as

well as one where  $M \sim |\mu|$  ( $M = 93$  GeV,  $\mu = -90$  GeV). We show in Fig. 4 the dependence of the SUSY-QCD correction (in % of the tree-level width) on the  $\tilde{t}_1$  mass in the range of  $m_{\tilde{t}_1} = 230$  to 400 GeV, for  $\cos \theta_{\tilde{t}} = 0.72$ . As in the case of the  $\tilde{t}_1 \rightarrow b \tilde{\chi}_1^+$  decay, the decay width gets the biggest correction if  $\tilde{\chi}_1^0$  is higgsino-like: It is between -30% and -20% and decreases with increasing  $\tilde{t}_1$  mass. For  $M \ll |\mu|$  ( $M \sim |\mu|$ ) the correction lies between  $\sim +8\%$  and  $\sim -5\%$  ( $\sim -3\%$ ).

The dependence of the tree-level (dashed lines) and the QCD corrected (solid lines) decay widths of  $\tilde{t}_1 \rightarrow t \tilde{\chi}_1^0$  on the stop mixing angle is shown in Fig. 5 for  $m_{\tilde{t}_1} = 260$  GeV and the other parameters as given in Fig. 4. Again there is a strong dependence on the nature of the lightest neutralino. The corrections are large for a higgsino-like neutralino.

Summarizing, we have computed the  $\mathcal{O}(\alpha_s)$  SUSY-QCD corrections to the decays of squarks into charginos and neutralinos. We have concentrated on the third generation squarks, where the quark masses cannot be neglected, and the left-right mixing plays an essential rôle. The corrections strongly depend on the nature of the charginos or neutralinos. They are about 10%, but go up to 40% for higgsino-like charginos/neutralinos.

## Acknowledgements

This work arose from the Workshop on Physics at LEP2, CERN 1995, and the Workshop on Physics with  $e^+e^-$  Linear Colliders, Annecy – Gran Sasso – Hamburg, 1995. This work was supported by the “Fonds zur Förderung der wissenschaftlichen Forschung” of Austria, project no. P10843-PHY.

## References

- [1] For a review, see:  
H.E. Haber, G.L. Kane, Phys. Rep. 117 (1985) 75
- [2] J. Ellis, S. Rudaz, Phys. Lett. B128 (1983) 248  
J.F. Gunion, H.E. Haber, Nucl. Phys. B272 (1986) 1
- [3] R. M. Barnett, J. F. Gunion, H. E. Haber, Phys. Rev. D37 (1988) 1892  
H. Baer, V. Barger, D. Karatas, X. Tata, Phys. Rev. D36 (1987) 96
- [4] H. Baer, X. Tata, J. Woodside, Phys. Rev. D42 (1990) 1568  
A. Bartl, W. Majerotto, B. Mösslacher, N. Oshimo, S. Stippel,  
Phys. Rev. D43 (1991) 2214  
A. Bartl, W. Majerotto, B. Mösslacher, N. Oshimo, Z. Phys. C52 (1991) 477
- [5] A. Bartl, W. Majerotto, W. Porod, Z. Phys. C 64 (1994) 499
- [6] A. Bartl, H. Eberl, S. Kraml, W. Majerotto, W. Porod, Vienna preprint, hep-ph/9603410,  
to be published in Z. Phys. C  
S. Ambrosiano et al., Conveners: G. F. Giudice, M. L. Mangano, G. Ridolfi, and R. Rückl,  
Proc. of the Workshop on Physics at LEP2, Vol. 1, p. 481, CERN 96-01, Editors: G.  
Altarelli, T. Sjöstrand, and F. Zwirner  
A. Bartl, H. Eberl, S. Kraml, W. Majerotto, W. Porod, A. Sopczak, Proc. of the Workshop  
on Physics with  $e^+e^-$  Liner Colliders, Annecy – Gran Sasso – Hamburg, 1995, Editor: P.  
Zerwas
- [7] H. Eberl, A. Bartl, W. Majerotto, Vienna preprint, hep-ph/9603206,  
to be published in Nucl. Phys.
- [8] K. Hikasa, Y. Nakamura, Z. Phys. C70 (1996) 139
- [9] A. Djouadi, W. Hollik, C. Jünger, Karlsruhe preprint, KA-TP-14-96, hep-ph/9605340
- [10] W. Beenakker, R. Höpker, P. M. Zerwas, DESY 96-022, hep-ph/9602378 (1996)
- [11] A. Bartl, H. Fraas, W. Majerotto, Nucl. Phys. B278 (1986) 1
- [12] A. Bartl, H. Fraas, W. Majerotto, B. Mösslacher, Z. Phys. C55 (1992) 257
- [13] G. Passarino and M. Veltman, Nucl. Phys. B160 (1979) 151
- [14] A. Denner, Fortschr. Phys. 41 (1993) 307
- [15] W. Siegel, Phys. Lett. B84 (1979) 193  
D. M. Capper, D. R. T. Jones, P. van Nieuwenhuizen, Nucl. Phys. B167 (1980) 479
- [16] Review of Particle Properties, Particle Data Group, Phys. Rev. D50 (1994)

## Figure captions

**Fig. 1:** Feynman diagrams relevant for the  $\mathcal{O}(\alpha_s)$  SUSY-QCD corrections to squark decays into charginos and neutralinos: (a) tree level, (b) gluon vertex correction, (c) gluino vertex correction, (d) and (e) quark wave-function renormalization, (f) and (g) squark wave-function renormalization, (h) four-squark interaction, and (i) and (j) real gluon emission.

**Fig. 2:** SUSY-QCD corrections for the decay  $\tilde{t}_1 \rightarrow b \tilde{\chi}_1^\pm$  in percent of the tree-level width as a function of  $m_{\tilde{t}_1}$  for  $m_{\tilde{\chi}_1^\pm} = 75$  GeV,  $m_{\tilde{t}_2} = 300$  GeV,  $m_{\tilde{b}_1} = 220$  GeV,  $m_{\tilde{b}_2} = 230$  GeV,  $\cos \theta_{\tilde{t}} = 0.72$ ,  $\cos \theta_{\tilde{b}} = -0.4$ ,  $\tan \beta = 2$ . Three scenarios are studied:  $M = 66$  GeV,  $\mu = -500$  GeV (solid line),  $M = 70$  GeV,  $\mu = -61$  GeV (dashed line), and  $M = 300$  GeV,  $\mu = -62$  GeV (dash-dotted line).

**Fig. 3:** Tree-level (dashed lines) and SUSY-QCD corrected (solid lines) widths of the decay  $\tilde{t}_1 \rightarrow b \tilde{\chi}_1^\pm$  in GeV as a function of  $\cos \theta_{\tilde{t}}$  for  $m_{\tilde{\chi}_1^\pm} = 75$  GeV,  $m_{\tilde{t}_1} = 150$  GeV,  $m_{\tilde{t}_2} = 300$  GeV,  $m_{\tilde{b}_1} = 220$  GeV,  $m_{\tilde{b}_2} = 230$  GeV,  $\cos \theta_{\tilde{b}} = -0.4$ ,  $\tan \beta = 2$ . Three scenarios are studied: (a)  $M = 66$  GeV,  $\mu = -500$  GeV, (b)  $M = 70$  GeV,  $\mu = -61$  GeV, and (c)  $M = 300$  GeV,  $\mu = -62$  GeV.

**Fig. 4:** SUSY-QCD corrections for the decay  $\tilde{t}_1 \rightarrow t \tilde{\chi}_1^0$  in percent of the tree-level width as a function of  $m_{\tilde{t}_1}$  for  $m_{\tilde{\chi}_1^0} = 50$  GeV,  $m_{\tilde{t}_2} = 500$  GeV,  $m_{\tilde{b}_1} = 320$  GeV,  $m_{\tilde{b}_2} = 340$  GeV,  $\cos \theta_{\tilde{t}} = 0.72$ ,  $\cos \theta_{\tilde{b}} = -0.4$ ,  $\tan \beta = 2$ . Three scenarios are studied:  $M = 98$  GeV,  $\mu = -500$  GeV (solid line),  $M = 93$  GeV,  $\mu = -90$  GeV (dashed line), and  $M = 250$  GeV,  $\mu = -55$  GeV (dash-dotted line).

**Fig. 5:** Tree-level (dashed lines) and SUSY-QCD corrected (solid lines) widths of the decay  $\tilde{t}_1 \rightarrow t \tilde{\chi}_1^0$  in GeV as a function of  $\cos \theta_{\tilde{t}}$  for  $m_{\tilde{\chi}_1^0} = 51$  GeV,  $m_{\tilde{t}_1} = 260$  GeV,  $m_{\tilde{t}_2} = 500$  GeV,  $m_{\tilde{b}_1} = 320$  GeV,  $m_{\tilde{b}_2} = 340$  GeV,  $\cos \theta_{\tilde{b}} = -0.4$ ,  $\tan \beta = 2$ . Three scenarios are studied: (a)  $M = 98$  GeV,  $\mu = -500$  GeV, (b)  $M = 93$  GeV,  $\mu = -90$  GeV, and (c)  $M = 250$  GeV,  $\mu = -55$  GeV.

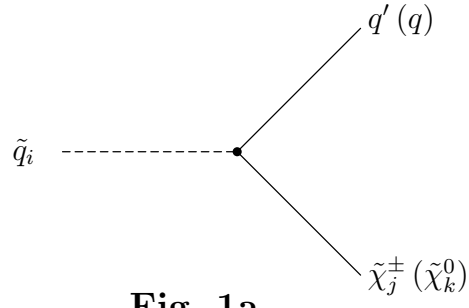


**Fig. 1a**

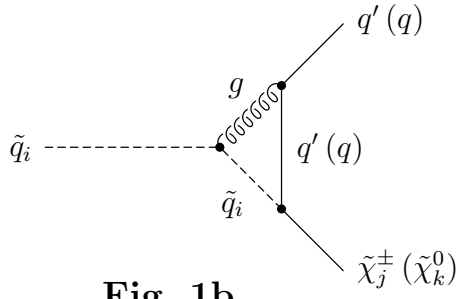


**Fig. 1b**

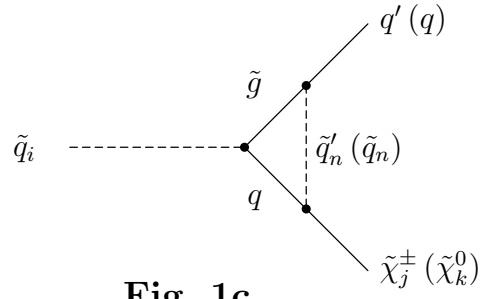


**Fig. 1c**

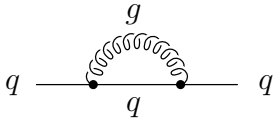


**Fig. 1d**

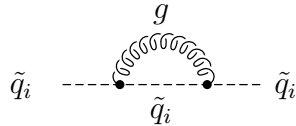


**Fig. 1f**

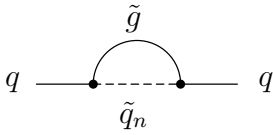


**Fig. 1e**

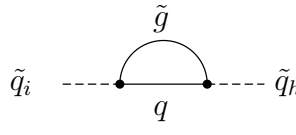


**Fig. 1g**

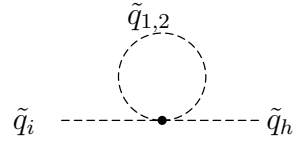


**Fig. 1h**

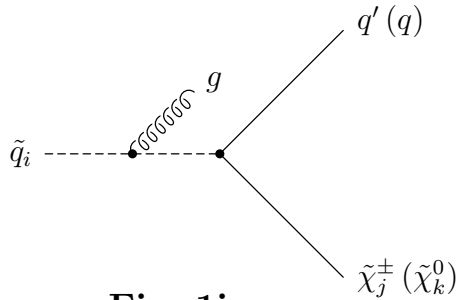


**Fig. 1i**

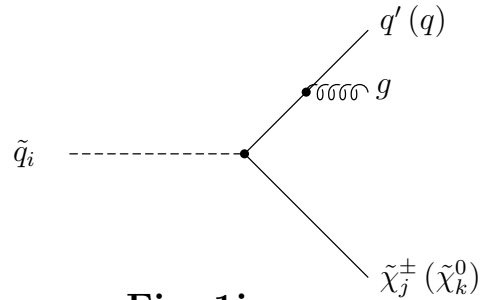


**Fig. 1j**

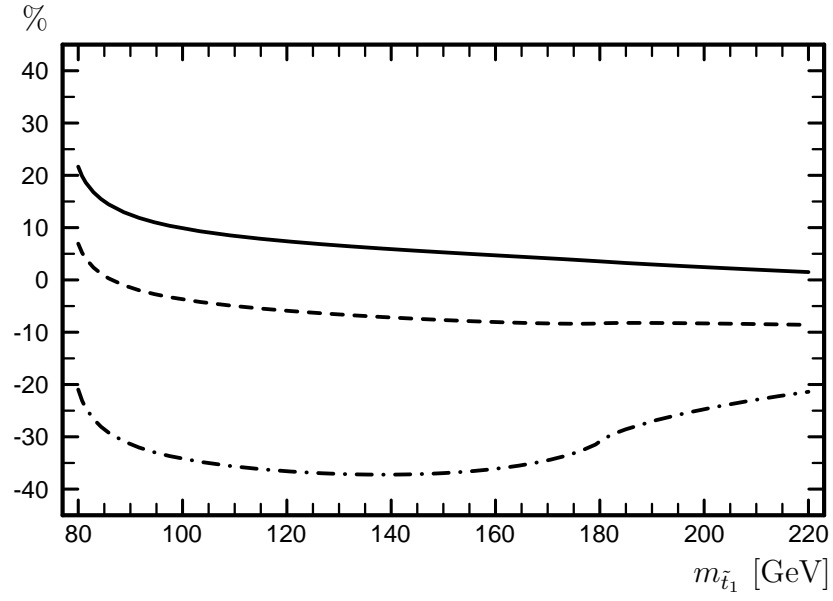


Fig. 2

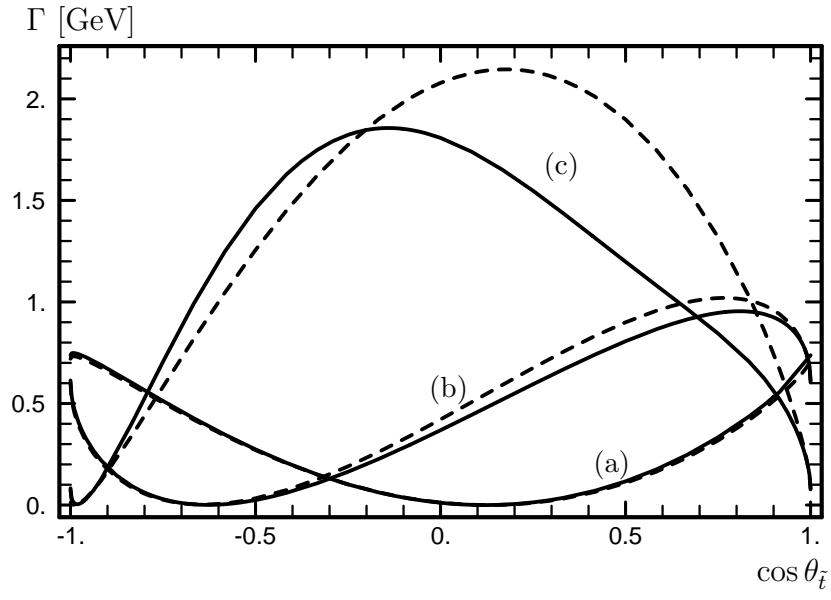


Fig. 3

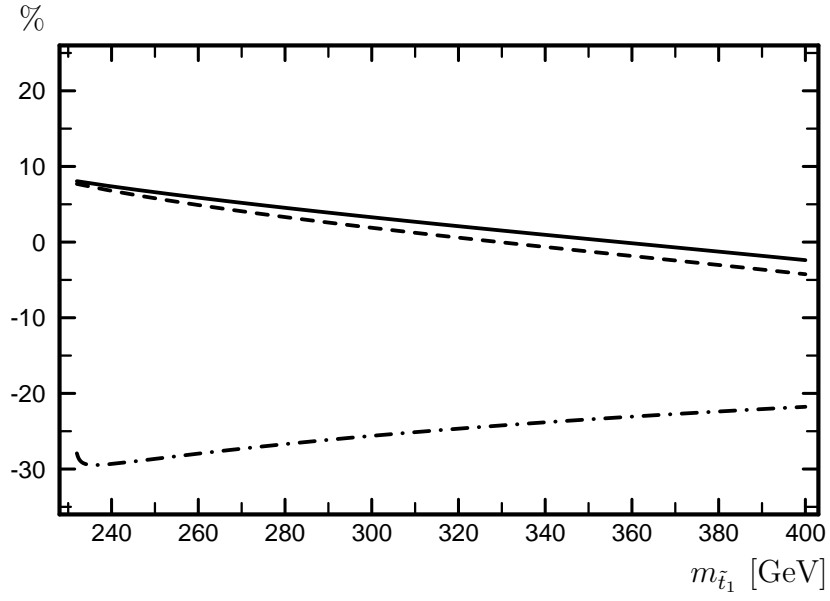


Fig. 4

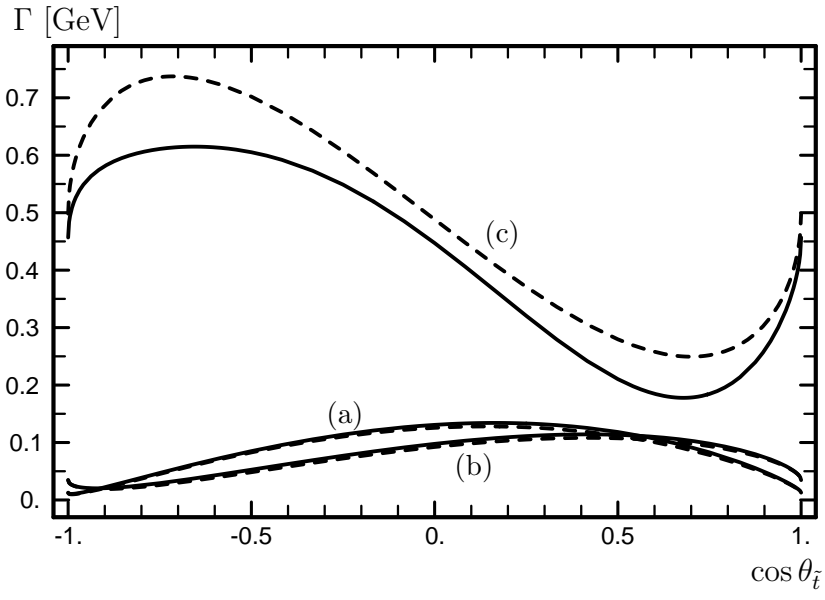


Fig. 5